CHAPTER FOURTEEN

Fluorescence Polarization Anisotropy to Measure RNA Dynamics

Xuesong Shi* *and* Daniel Herschlag[†]

Contents

* Department of Biochemistry, Stanford University, Stanford, California, USA
† Departments of Biochemistry and Chemistry, Stanford University, Stanford, California, USA

Abstract

RNA requires helical motion to fold and carry out its function. As RNA helical motion occurs on the nanosecond timescale, the timescale probed by fluorescence dyes, fluorescence polarization anisotropy (FPA) is a simple, yet powerful, technique to study helical dynamics in RNA. With the recent development of several fluorescent base analogs that have a nanosecond timescale lifetime in a duplex, FPA has begun to be used for characterizing RNA dynamics. Using the probe 6-methylisoxanthopterin (6-MI) as an example, we describe the procedure for carrying out FPA experiments on model oligonucleotide systems and in a complex RNA, the *Tetrahymena* group I intron. For smaller RNA systems, isolating the motion of the target helix from the overall tumbling of the whole RNA system is necessary, and nucleic acids binding proteins can be incorporated into the RNA system to increase the overall size of the system, slow the overall tumbling, and thereby reduce the anisotropy contribution from the overall tumbling to negligible. The procedure for incorporating one such protein, the Lac Repressor, is given as an example.

1. INTRODUCTION

Like other macromolecules, RNA is dynamic. The process of folding into a structured RNA involves dynamic rearrangement of RNA helices, and many RNAs function via a series of conformational transitions. Thus, measurement of the dynamics of individual helices will be required to fully understand RNA folding and function. Additionally, dynamic information can also be used to provide information about local structural features.

As the movements of individual helices are often on the nanosecond timescale, fluorescence polarization anisotropy (FPA) (Bucci and Steiner, 1988; Duhamel et al., 1996; LiCata and Wowor, 2008; Thomas et al., 1980) is a natural choice for studying RNA dynamics; FPA measures the rate of depolarization of a fluorophore during its lifetime, which is often in the low nanosecond regime. Despite its potential, FPA has been rarely used for studying RNA dynamics, largely due to a lack of suitable probes. With the recent development of several new fluorescent base analogs, wider application of the FPA technique for measuring RNA dynamics has become possible (Shi et al., 2009). Besides FPA, NMR and EPR have both been successfully used in characterizing RNA dynamics on the nanosecond timescale (Edwards and Sigurdsson, 2007; Grant et al., 2009; Zhang et al., 2006, 2007). The fluorescence-based FPA methods complement NMR and EPR well in that FPA is not limited by the size of the RNA being studied and does not require large amount of samples as NMR, is a more direct readout of dynamics, involves relatively inexpensive equipment, and is potentially applicable to transient intermediates due to its high time resolution.

2. General Information of FPA Measurement

2.1. L-format and T-format

Fluorescence anisotropy is normally measured as

$$r = \frac{I_{VV} - (I_{HV}/I_{HH})I_{VH}}{I_{VV} + 2(I_{HV}/I_{HH})I_{VH}}. \tag{14.1}$$

In Eq. (14.1), I is fluorescent intensity; the subscript letters, V for vertical and H for horizontal, represent the polarization direction of the two polarizers on the excitation and emission light path, respectively; and the ratio, I_{HV}/I_{HH}, calibrates for the difference in the emission channel's sensitivity towards vertical and horizontal polarized components. Anisotropy, r, can be measured by either L-format or T-format. In the L-format, all four fluorescence intensities, I_{VV}, I_{VH}, I_{HV}, and I_{HH}, are measured using a single channel of a photodetector so that each intensity needs to be measured separately. If the fluorimeter has two emission channels then anisotropy can also be measured in a T-format, which allows fluorescence intensities pairs, I_{VV}/I_{VH} or I_{HV}/I_{HH}, to be measured simultaneously via the two emission channels. Thus, measurements in the T-format are faster than in the L–format.

2.2. Determining anisotropy and minimizing background signal

To obtain the correct anisotropy of the dye, background signals from the buffer solution and macromolecule solutes must be factored out. The anisotropy signal from the dye is determined using background corrected values of I_{VV}, I_{VH}, I_{HV}, and I_{HH}, which are obtained by subtracting the intensities of reference samples that contain all of the components of the real sample, except the dye, from measured sample intensities. This procedure minimizes the background signal's contribution to the uncertainty in anisotropy values. It is desirable to optimize the buffer condition to minimize background signal. All sample components should preferably produce very small fluorescence signal (via fluorescence or scattering) relative to the fluorophore signal. If the background signal is strong, each component in the buffer solution should be tested for fluorescence in water at the experimental wavelength. The high–signal components should be replaced or used at lower concentration.

2.3. Choosing a wavelength for anisotropy measurement

To find the optimum excitation wavelength for an anisotropy measurement, the excitation wavelength dependence of anisotropy (r) is plotted to determine the range of excitation wavelengths, λ_{ex}, that give a constant

value of r. The excitation wavelength that is used should be well within this range and give the strongest emission intensity, unless there are additional complicating features of the system, such as much greater background contributions at the maximum emission wavelength.

2.4. Testing polarizer alignment

The alignment of polarizers should be tested periodically to maintain data accuracy and consistency. We dilute glycogen (Sigma; cat. #G8751) solution until it reaches a stable maximum anisotropy. The scattered light from diluted glycogen solution is 100% polarized with r equal to 1 (Lakowicz, 2006). We consider the alignment to be satisfactory if the maximum anisotropy is larger than 0.98. A stock glycogen solution of the final diluted concentration is kept at $-20\,^{\circ}$C for future testing. The glycogen solution should not be overdiluted, otherwise there can be effects from background signal.

2.5. Factors that influence anisotropy

Consider the simplest case in which a dye molecule is rigidly attached to a spherical macromolecule. If the dye molecule has a single exponential decay in its lifetime then the expected steady anisotropy is

$$r = \frac{r_0}{1 + (\tau/\theta)} \tag{14.2}$$

where r_0 is the fundamental anisotropy, which is related to the angle between the absorption and emission dipoles of the dye, and $\theta = \eta V/RT$, where η is viscosity, V is the hydrodynamic volume, R is the gas constant, T is temperature, and θ is the rotational correlation time. Given knowledge of r_0 and τ, the fluorescence lifetime of the dye, information about the rotational dynamics of the macromolecule, θ, can be obtained from the observed anisotropy. In practice, the attachment of the dye to the macromolecule is often not completely rigid. When the segmental motion of the fluorophore is much more rapid than the tumbling of the macromolecule, such motion can simply be represented by using apparent fundamental anisotropy, r_0^{app}, instead of r_0, where $r_0^{\mathrm{app}} < r_0$. The value of r_0^{app} can be obtained by measuring anisotropy with increasing viscosity of the solution, such that at high enough viscosity, the term $r/\theta = \tau RT/\eta V$ approaches zero and

$$r_{\mathrm{obs}} = \frac{r_0^{\mathrm{app}}}{1 + (\tau/\theta)} \tag{14.3}$$

approaches r_0^{app}. The observed anisotropy, r_{obs} is influenced by the properties of the dye, r_0^{app} and τ, as well as solution properties, η and T. All these parameters are needed to relate r_{obs} to macromolecule motion.

3. Choice of FPA Probes

One of the main advantages of using a fluorescent base analog over other fluorescent dyes is that the movement of fluorescent base analog can be strongly coupled with the labeled RNA helices through base pairing with the complementary base in the helix and base stacking. Such strong couplings allow the dynamics of the RNA helices to be relatively directly reported by the FPA of the base analogs. Specifically, labeling RNA with regular fluorescent dyes often requires a covalent linker. This linker reduces the motional coupling between the RNA and dye and convolutes the interpretation of FPA data with potential linker–RNA interactions. Although dyes that are intercalators, such as ethidium bromide, can achieve strong coupling with RNA in its motion, binding of intercalator dyes is not sequence specific and introduces significant structural changes in RNA. In contrast, fluorescent base analogs introduce little perturbation to RNA structure.

To be used as a FPA probe for RNA helical dynamics, a fluorescent base analog also needs to maintain a significant level of fluorescence intensity and a lifetime on the nanosecond timescale once incorporated into a duplex. Only a small fraction of the reported fluorescence base analogs (Asseline, 2006; Rist and Marino, 2002; Wilson and Kool, 2006) satisfy this criteria; notable examples include 6-methylisoxanthopterin (6-MI), 1,3-diaza-2-oxophenothiazine (tC), and 1,3-diaza-2-oxophenoxazine (tC°) (Hawkins et al., 1997; Sandin et al., 2005, 2008; Wilhelmsson et al., 2001) (Fig. 14.1). The fluorescent properties of these three dyes are summarized in Table 14.1. As more accurate measurements of anisotropy can be achieved with a higher ratio of dye intensity to background signal, it is desirable to use a brighter dye and a dye that emit at a wavelength far from the absorption maximum of RNA, thereby minimizing the background signal from the natural bases. All three dyes noted above are reasonably bright at excitation wavelengths that are well distanced from the absorption maximum of the natural bases. The maximum excitation wavelength for 6-MI, tC°, and tC monomers are 340, 360, and 375 nm, respectively. Although tC has the most red–shifted excitation wavelength, it is about three times less bright in
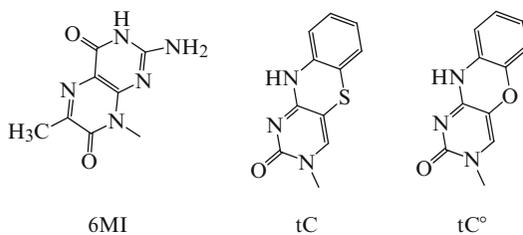

Figure 14.1 Structures of 6-MI, tC, and tC°.

Table 14.1   Fluorescence properties of 6-MI, tC, and tC° incorporated in an RNA (6-MI) or DNA duplex (tC and tC°)

	Quantum yield	Lifetime (ns)	Extinction coefficient of free nucleoside (M^{-1} cm^{-1})
6-MI[a]	0.21	4.4 (Bucci and Steiner, 1988)	$\varepsilon_{340} \sim 4350$ (Hawkins et al., 1997)
tC	0.18–0.21 (Sandin et al., 2005)	5.9–6.9 (Sandin et al., 2005)	$\varepsilon_{375} = 4000$ (Wilhelmsson et al., 2003)
tC°	0.17–0.27 (Sandin et al., 2008)	3.5–4.8 (Sandin et al., 2008)	$\varepsilon_{360} = 9000$ (Sandin et al., 2008)

[a] In the sequence 5′-CUFUC-3′, where F = 6-MI, base paired to its complement.

a duplex than tC° (Sandin et al., 2008). 6-MI can be as bright as tC° within specially designed sequences. One advantage of tC and tC° over 6-MI is that fluorescent properties of tC° and especially tC are less sensitive to the neighboring base sequences than 6-MI. This reduced sensitivity allows tC° and tC to be incorporated into RNA with a minimum degree of sequence design and alteration. The main advantage of 6-MI over tC° and tC is that 6-MI-modified oligos are commercially available (Fidelity Systems Inc., Gaithersburg, MD). Procedures for synthesizing and incorporating of all three dyes are available in the literature (Hawkins, 2007; Sandin et al., 2007, 2008). The protocols given in the following section are based on using 6-MI as the labeling dye.

4. Measuring FPA in a Simple Duplex, using an 11mer Control RNA Duplex as an Example

4.1. Sequence design

The ideal RNA sequence surrounding 6-MI in an oligonucleotide is YUFUY, where F is 6-MI and Y is a pyrimidine. Exchanging the neighboring U to other nucleotides (except T) or exchanging Y to G can shorten the lifetime of 6-MI to the subnanosecond timescale (Hawkins et al., 1997).

4.2. Sample preparation

6-MI-containing 11mer RNA oligonucleotides were obtained from Fidelity Systems (Gaithersburg, MD). Oligonucleotides were purified by ion exchange HPLC on a DNAPAC PA100 column (Dionex, Sunnyvale, CA)

using a linear gradient of 10 mM to 2 M ammonium acetate, pH 5.5, in 10% acetonitrile. The collected fractions were dried in a speed–vac overnight to remove residual salt and then resuspended in 50 μL TE buffer (25 mM Tris–HCl, 0.1 mM EDTA, pH 8.0) for long-term storage at -20 °C.

Note: 6–MI–containing oligonucleotides can also be made following a literature protocol (Hawkins, 2007).

Note: If the experiments are highly sensitive to salt, then it is recommended to desalt the oligonucleotides by a reverse phase cartridge, such as a C-18 sep–Pak cartridge from Waters (Milford, MA), before speed–vac concentrating. Alternatively, the HPLC-purified oligonucleotides can be desalted and concentrated by ethanol precipitation.

The 6–MI–labeled 11mer oligonucleotide is annealed with an excess amount of the complementary strand at a molar ratio of 1:5 at 95 °C for 2 min before gradually cooling to room temperature over 30 min. The completion of hybridization can be checked by native 15% polyacrylamide gel electrophoresis (15% for 10–25 bp in a duplex). The mixture is diluted to a final concentration of 100–200 nM of the 6–MI strand in 50 mM NaMOPS, pH 7.0, with the desired amount of added salt before FPA measurements. A minimum concentration of 100 nM 6-MI is suggested to maintain a ratio of dye intensity to background that is sufficiently high.

4.3. FPA measurement

We performed FPA measurements on a Fluorolog-3 spectrometer from Horiba Jobin Yvon (Edison, NJ) using L-format. For 6-MI studies, excitation and emission wavelengths were set to 350 and 425 nm, respectively. As anisotropy is relatively sensitive to temperature, a water bath is connected to the sample compartment for temperature control. The first measurement is made after incubation in the sample compartment for 10 min to allow for temperature equilibration. For each measurement, the average of three consecutive readouts of anisotropy and fluorescent intensities is recorded, and three to four of such measurements are made over $\sim$10 min to ensure that the solution is well equilibrated and that there is no time dependence in the anisotropy. Each anisotropy value obtained is corrected for the background by calibrating the four intensities, I_{VV}, I_{VH}, I_{HV}, and I_{HH}, with background intensities separately; for example, $I_{VV} = I_{VV,observed} - I_{VV,background}$. Then the anisotropy is calculated using the corrected intensities as Eq. (14.1). The three to four corrected anisotropy values are averaged to give a value with a standard deviation that is generally smaller than 0.002. Results from two to four independent samples measured on at least 2 different days are averaged to give the final anisotropy value. With all anisotropy values pooled, the standard deviation is generally smaller than 0.0025.

5. Use of FPA to Study Helical Dynamics of RNA, with a Junction Model Construct as an Example

RNA structure is largely composed of helical segments connected by various kinds of junctions. Here, we broadly define a junction as any non-Watson Crick base-paired region. With the properly base-paired helical segments being relatively rigid, the flexibility in RNA predominately comes from the junction regions. The effects of different types and sequences of junctions on helical dynamics can be studied individually by using a minimal construct consisting of a dye-labeled helix connected to a nonlabeled helix through the target junction. Thus, the impact of junctions on the motion of the labeled helix can be assessed by FPA.

However, the observed anisotropy is determined from depolarization of the dye, which can arise from not only the junction-modulated movement of dye-labeled helix but also from the overall tumbling of the RNA molecule. One way to separate the desired junction-modulated motion from overall tumbling is to increase the overall size of the construct, thereby rendering overall tumbling too slow to cause any significant depolarization over the lifetime of the dye so that the contribution of tumbling to the observed anisotropy is negligible. To increase the construct size, we extended the nonlabeled helix to include a 20-bp LacI operon DNA sequence, which allowed us to bind the 154 kDa Lac Repressor (LacI). (This protein is equivalent to about a 320-bp DNA duplex in volume (Chalikian and Breslauer, 1998; Fischer *et al.*, 2004).) Construction and FPA measurement of model systems consisting of single-stranded AAA (A_3) and UUU (U_3) junctions are described in Scheme 14.1.

5.1. Assembling the constructs without LacI

The A_3 and U_3 constructs were assembled from two single-stranded oligos, an 11mer short strand and a 50mer long strand (Scheme 14.1). The short strand contains 6-MI and the long strand contains the LacI operon sequence. The long strand was obtained from Integrated DNA Technologies (Coralville, IA) and purified by denaturing polyacrylamide gel electrophoresis.

The constructs (Scheme 14.1) were assembled in two steps. In the first step, the purified partially self-complementary long strand was annealed at 95 °C for 5 min, gradually cooled to 50 °C over 40 min and then quickly cooled on ice to form a duplex with short hangover regions on both sides.

Note: The long strand is partially self-complementary (The 36 nt sequence at the 3′-end of the 50mer is self-complementary, Scheme 14.1), and this property reduces the number of oligos that need to be purchased. However,

```
Duplex constructs*
        5′-r(GGACAGGAGGG -X - AGUUA)d(GCGAATTGTGAGCGCTCACAATTCGC)r(UAACU)     r(CCCUCCUFUCC)-3′
        3′-r(CCUFUCCUCCC)      (UCAAU)d(CGCTTAACACTCGCGAGTGTTAAGCG)r(AUUGA) - X - GGGAGGACAGG-5′

        Construct A₃ : X = AAA
        Construct U₃ : X = UUU
Construct segments
        Short strand (11 mer): 5′-r(CCCUCCUFUCC)-3′        F = 6-MI
        Long strand  (50 mer): 5′-r(GGACAGGAGGG-AAA-AGUUA) d(GCGAATTGTGAGCGCTCACAATTCGC)r(UAACU)
                               5′-r(GGACAGGAGGG-UUU-AGUUA) d(GCGAATTGTGAGCGCTCACAATTCGC)r(UAACU)

        The Lacl operon sequence is underlined.
        *r(...) represents RNA
        d(...) represents DNA
```

Scheme 14.1 Example constructs with single-stranded AAA and UUU junction.

the disadvantage of having a partially self-complementary sequence is the possibility of forming alternative stable hairpin structures. After proper annealing, the purity of the annealed complex should be assessed by non-denaturing gel electrophoresis. In our case there were negligible amounts (2–4%) of hairpin. High oligonucleotide concentration in the annealing step can help favor intermolecular complex formation.

In the second step, 5 μM of the annealed long strand duplexes were hybridized with 2 μM short strand at 38 °C for 30 min. Complete hybridization (>98%) was confirmed by nondenaturing gel electrophoresis.

The mixture was diluted to a final concentration of 100 nM short strand and 250 nM long strand duplexes for FPA measurement. Excess annealed long strand duplexes can be added to ensure that there is no further increase in anisotropy, as this species does not contain the fluorescence dye.

5.2. Lac Repressor (LacI)

5.2.1. Transformation

Add 1 μL Plasmid pMDB1 (a gift from Michael Brenowitz, Albert Einstein College of Medicine) into 100 μL competent BL21-DE3-pLysS cells (Promega, Madison, WI). Incubate the mixture on ice for 30 min, then heat shock the sample at 42 °C for 90 s to allow plasmid uptake. After the heat shock, immediately ice the sample for another 2 min. Add 1 mL LB media to the cells and grow for 1 h at 37 °C with shaking. Use microbeads to spread cells evenly onto a LB agarose plate prewarmed at 37 °C containing Carbenicillin and Chloramphenicol, which will select for cells that have taken up the plasmid. Grow at 37 °C overnight.

On the second day, there should be identifiable colonies growing on the plate. Cover the plate with parafilm and store at 4 °C to avoid overgrowth of colonies. Before the end of the day, pick a colony from the plate and add the colony into 100 mL LB together with 100 μL of 50 mg/mL Carbenicillin and 100 μL of 10 mg/mL Chloramphenicol, then grow overnight at 37 °C with shaking.

5.2.2. Cell growth and induction

Pellet cells for 5 min in two 50 mL Falcon tubes (e.g., 2000 rpm in a Beckman J-6M swinging bucket centrifuge with Beckman JS-4.2 rotor). (We use sterile Falcon tubes (BD Biosciences, San Jose, CA, cat. #352070) to minimize the chance of nuclease contamination.) The supernatant is removed. Optionally, one pellet can be resuspended in equal volume of LB (1% Bacto Tryptone, 0.5% yeast extract and 0.5% NaCl in water) and 60% glycerol, divided into multiple fractions and stored at −80 °C for future use. The other pellet is resuspended in 25 mL at 37 °C LB, then add into 2 L LB containing 2 mL of 50 mg/mL Carbenicillin and 2 mL of 10 mg/mL Chloramphenicol. Grow at 37 °C until the OD_{600} is close to 1,

which normally takes about 4–6 h. Remove 1 mL for SDS–PAGE. Add 0.2 mL 1 M IPTG to a final concentration of 0.1 mM to induce gene expression, continue to grow for another 2 h at 37 °C. Remove 1 mL for SDS–PAGE analysis of the amount of LacI products. The result of IPTG induction is tested by 12% SDS–PAGE. An aliquot (100 μL) from each of the two 1 mL pre-IPTG and after-IPTG samples are centrifuged for 5 min at 18,500×g. The pellets are resuspended in 14 μL of gel loading buffer and incubated at 90 °C for 6 min before loading onto the gel. If the IPTG induction is successful, the after-IPTG lane should have a strong band at around 38.5 kDa, the molecular weight of LacI monomer, and this band should be much weaker in the pre-IPTG lane. Centrifuge the after-IPTG cells in two 1 L centrifuge bottles at 4500 × g for 15 min, remove supernatant, resuspend in 0.01 M Tris–HCl, pH 8.0, transfer to 50 mL Falcon tubes, centrifuge for 7 min at 4500 × g, remove supernatant and freeze the pellets at −80 °C.

5.2.3. Cell lysis

The frozen pellets are thawed on ice, then resuspended in buffer A (25 mM Bis–Tris, pH 6.0, 1 mM MgCl$_2$, 1 mM DTT, 15% glycerol, and 150 mM KCl). The cell suspension is lysised by French press at 1100 psi two to three times. The lysed samples are centrifuged at 38,000×g for 20 min at 4 °C. The supernatant is transferred to a fresh tube, and the DNA is precipitated by adding protamine sulfate (6 mg/mL) while stirring to a final concentration of 0.3 mg/mL. The sample is centrifuged at 38,000×g for 20 min at 4 °C. The supernatant is decanted and buffer exchanged with buffer A using Amicon Ultra-15 concentrator (Millipore, Billerica, MA) with a molecular weight cutoff of 10 kDa.

5.2.4. FPLC purification

The sample solution is first purified using a HiTrap SP HP (GE Healthcare Bio-Sciences, Piscataway, NJ) cation exchange column using buffer A as the starting buffer and buffer B (25 mM Bis–Tris, pH 6.0, 1 mM MgCl$_2$, 1 mM DTT, 15% glycerol, and 2 M KCl) as the elution buffer. The samples are eluted with a linear gradient of 150–650 mM KCl over 6 min at 5 mL/min. The LacI peak elutes at 380–420 mM KCl. The amount and purity of LacI in each collected fraction can be tested by 12% SDS–PAGE.

The main LacI containing fractions are pooled and then further purified over a HiPrep 16/60 Sephacryl 200 (Pharmacia Biotech, now GE Healthcare Bio-Sciences) gel filtration column preequilibrated with the running buffer C (25 mM Tris–HCl, pH 8.0, 1 mM EDTA, 1 mM DTT, 15% glycerol, and 600 mM KCl). Load no more than 5 mL of sample per run for a HiPrep 16/60 Sephacryl 200 column (5 mL is 1/24 of the column bed volume of 120 mL). The column is run at 1 mL/min with buffer C. The elution profile contains a smaller peak at around 26–34 mL and a larger peak

around 40–56 mL. The latter peak is identified as LacI by SDS–PAGE. The fractions collected of the latter peak are concentrated to about 200 μL with Amicon Ultra-15 concentrator (Millipore) with a molecular weight cutoff of 10 kDa. The concentrated solution is diluted three times with 25 mM Tris–HCl, pH 8.0, then further diluted with 10 mL of storage buffer (25 mM Tris–HCl, pH 8.0, 0.1 mM EDTA, 5% glycerol, and 200 mM NaCl). The solution is concentrated to about 200 μL and stored in 20 μL aliquots at $-80\,^\circ$C after measuring its absorbance. The concentration of LacI tetramer is calculated with an extinction coefficient of 0.10 μM^{-1} cm^{-1} at 280 nm.

Note: With 5% glycerol, the stock LacI solution is viscous. It is desirable to control the final glycerol concentration to be less than 0.5% or, in the other words, to concentrate the stock LacI solution to be at least 10 times more than the experimental LacI concentration. We concentrate LacI to 30 μM (OD$_{280}$ = 3) or above. Introduction of 0.5% glycerol increases the viscosity of the solution by slightly less than 1% and gives a negligible increase in the anisotropy of <1%.

5.3. Assembling model constructs with LacI and carrying out FPA measurements

Concentrated LacI solution is thawed on ice. After adjusting to the experimental salt concentration, the solution is vortexed briefly followed by centrifugation for 1 min at 16,000×g. The clear solution is transferred to a separate tube and kept on ice.

The annealed sample mixture of 100 nM short strand and 250 nM long strand duplex is titrated with the concentrated LacI until the anisotropy saturates (Fig. 14.2). The buffer condition is 50 mM NaMOPS, pH 7.0, and 280 mM added NaCl, for a total Na$^+$ concentration of 300 mM. Measure anisotropy as described in Section 4.

Note: Experiments with LacI were carried out with a salt concentration of 300 mM Na$^+$ or more to weaken the nonspecific LacI DNA binding, as nonspecific binding can affect FPA values. As nonspecific LacI DNA binding is associated with the release of several counterions, the K_d of nonspecific LacI DNA binding is strongly salt dependent. From literature data (Frank *et al.*, 1997), the dissociation constant for nonspecific LacI binding weakens from about 0.6($\pm$0.4) μM at 150 mM K$^+$ to about 41 ($\pm$16) μM at 300 mM K$^+$ at 15 $^\circ$C. Oversaturating the solution with LacI will increase the free LacI concentration, which results in more nonspecific LacI binding. Thus, it is desirable to limit the LacI concentration to be no more than 1 μM over the saturation value.

Note: During and after the LacI measurement, check the cuvette to make sure the solution remains clear over the entire experiments. Clouding is often an indication of LacI aggregation. This observation also typically gives
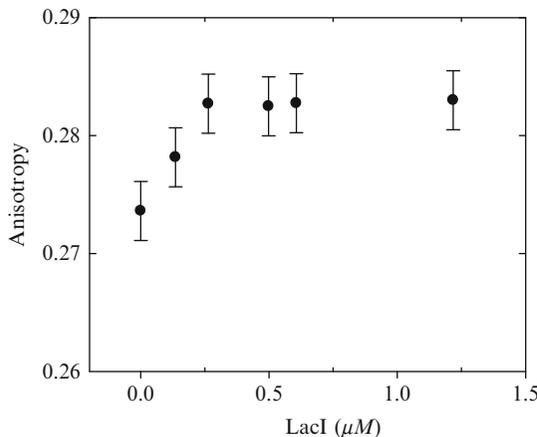
Figure 14.2 Titration of oligonucleotide model construct with increasing LacI. Conditions: 50 mM NaMOPS, pH 7.0, 280 mM NaCl, 15 °C with 100 nM of 6-MI-containing short strands and 250 nM of long strand duplex.

time–dependent fluorescence anisotropy values. If there is LacI aggregation, redo the experiments with freshly made buffer solutions.

6. USE OF FPA TO STUDY HELICAL DYNAMICS IN A COMPLEX RNA, WITH THE *TETRAHYMENA* GROUP I INTRON RIBOZYME AS AN EXAMPLE

Dynamics of individual helices of complex RNAs can be directly characterized by FPA by incorporating 6-MI into the target helix, provided that the complex RNA is large enough that its overall tumbling is much slower than the lifetime of 6-MI. The *Tetrahymena* group I ribozyme, roughly 400 nt in size, is one such RNA. The following protocol is for characterizing the dynamics of the P1 duplex in this ribozyme. The P1 duplex consists of an internal guidance strand (IGS) and a complementary substrate strand. The IGS strand connects to the rest of the ribozyme through a single-stranded junction, and the P1 duplex is formed by hybridizing the substrate strand, which is labeled with 6-MI, with the IGS (Fig. 14.3).

1. L–16 *ScaI* ribozyme was prepared by *in vitro* transcription with T7 RNA polymerase at 30 °C for 40 min in the presence of 4 mM MgCl$_2$, NTPs (0.5 mM each), 40 mM DTT, 2 mM spermidine, 40 mM Tris–HCl, pH 8.0, and 0.01% Triton X–100 (Karbstein *et al.*, 2007). The transcription product was then purified by 8% denaturing polyacrylamide gel electrophoresis.
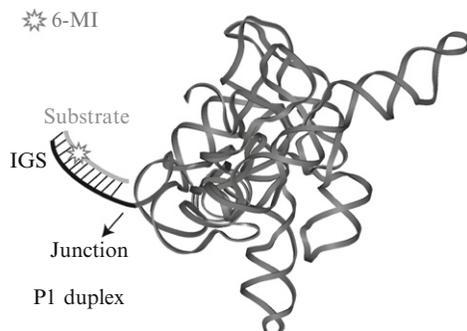
Figure 14.3 The *Tetrahymena* group I ribozyme and its P1 duplex. The P1 duplex consists of an internal guide sequence (IGS) and an oligonucleotide substrate, which can be conveniently labeled with 6-MI.

2. After purification, the ribozyme was folded at 50 °C for 30 min in 50 mM NaMOPS, pH 7.0, and 10 mM MgCl$_2$ (Bartley *et al.*, 2003). The folded solution was then buffer exchanged into the experimental buffer condition using the YM30 (30 kDa cutoff) Microcon centrifugal filter (Millipore) by concentrating from about 500 to 10–20 μL three times. The concentration of the folded ribozyme is determined by absorbance at 260 nM (using a NanoDrop ND-1000 Spectrophotometer, Thermo Fisher Scientific, Waltham, MA).

3. The concentrated ribozyme solution was annealed with concentrated 6-MI labeled substrate strands under the experimental buffer condition in a 4:1 molar ratio of ribozyme to substrate for 30 min at 38 °C. The annealed solution was then diluted to 200 nM of 6-MI and 0.8 μM ribozyme for FPA measurement. To ensure the sample has properly hybridized, the annealed solution was titrated with the concentrated ribozyme solution to a final ribozyme concentration, typically 2 μM, to ensure the saturation of FPA signal. FPA was measured as in Section 4.

Note: Alternatively, the folded ribozyme can be mixed with the 6-MI labeled substrate strands in a 3:1 ratio and annealed at 38 °C for 30 min. The annealed mixture can then be buffer exchanged with the experimental buffer using YM30 (30 kDa cutoff) Microcon centrifugal filter (Millipore) by concentrating from about 500 to 10–20 μL three times. This buffer exchange step also removes any substrate strand not associated with the ribozyme. After measuring concentration, the concentrated mixture can be used for FPA measurement by dilute to a final ribozyme concentration of 0.5 μM or higher. The obtained anisotropy is the same, within error (0.005), as that obtained by the above protocol.

Structured RNAs that are significantly smaller than the *Tetrahymena* ribozyme can be studied in the same way as a model oligonucleotide

construct by extending the structured RNA to include a LacI operon sequence or an RNA binding protein recognition sequence and increasing the size of the RNA by binding the corresponding protein to it.

7. Salt Dependence and Normalization of FPA with a Short Control Duplex

FPA results obtained at different salt conditions may not be directly comparable because the fluorescence properties of 6-MI, including the lifetime (τ), are salt dependent. The salt dependence of the FPA of a helix in a complex construct should thereby be normalized relative to the FPA of a short control duplex of the same sequence of the targeted helix to account for salt effects on the local environment of the 6-MI fluorophore. The normalization ratio, r_{norm}, can be calculated as the ratio between the apparent rotational correlation time, θ, of the constructs and the control duplex only, $r_{norm} = \theta_{construct}/\theta_{control}$. θ is related to the rate of anisotropy decay, with larger θ associated with higher anisotropy. If the basic Perrin equation for a sphere (Eq. (14.3)) is used to simplify calculation, then

$$ r_{norm} = \frac{(r_1^{app}/r_{control}) - 1}{(r_1^{app}/r_{construct}) - 1}. $$

ACKNOWLEDGMENTS

REFERENCES

Asseline, U. (2006). Development and applications of fluorescent oligonucleotides. *Curr. Org. Chem.* **10,** 491–518.

Bartley, L. E., Zhuang, X. W., Das, R., Chu, S., and Herschlag, D. (2003). Exploration of the transition state for tertiary structure formation between an RNA helix and a large structured RNA. *J. Mol. Biol.* **328,** 1011–1026.

Bucci, E., and Steiner, R. F. (1988). Anisotropy decay of fluorescence as an experimental approach to protein dynamics. *Biophys. Chem.* **30,** 199–224.

Chalikian, T. V., and Breslauer, K. J. (1998). Volumetric properties of nucleic acids. *Biopolymers* **48,** 264–280.

Duhamel, J., Kanyo, J., DinterGottlieb, G., and Lu, P. (1996). Fluorescence emission of ethidium bromide intercalated in defined DNA duplexes: evaluation of hydrodynamic components. *Biochemistry* **35,** 16687–16697.

Edwards, T. E., and Sigurdsson, S. T. (2007). Site-specific incorporation of nitroxide spin-labeles into 2′-position of nucleic acids. *Nat. Protoc.* **2,** 1954–1962.

Fischer, H., Polikarpov, I., and Craievich, A. F. (2004). Average protein density is a molecular-weight-dependent function. *Protein Sci.* **13,** 2825–2828.

Frank, D. E., Saecker, R. M., Bond, J. P., Capp, M. W., Tsodikov, O. V., Melcher, S. E., Levandoski, M. M., and Record, M. T. (1997). Thermodynamics of the interactions of lac repressor with variants of the symmetric lac operator: Effects of converting a consensus site to a non-specific site. *J. Mol. Biol.* **267,** 1186–1206.

Grant, G. P. G., Boyd, N., Herschlag, D., and Qin, P. Z. (2009). Motions of the substrate recognition duplex in a group I intron assessed by site-directed spin-labeling. *J. Am. Chem. Soc.* **131,** 3136–3137.

Hawkins, M. E. (2007). Synthesis, purification and sample experiments for fluorescent pteridine-containing DNA: Tools for studying DNA interactive systems. *Nat. Protoc.* **2,** 1013–1021.

Hawkins, M. E., Pfleiderer, W., Balis, F. M., Porter, D., and Knutson, J. R. (1997). Fluorescent properties of pteridine nucleoside analogs as monomers and incorporated into oligonucleotides. *Anal. Biochem.* **244,** 86–95.

Karbstein, K., Lee, J., and Herschlag, D. (2007). Probing the role of a secondary structure element at the 5′- and 3′-splice sites in group I intron self-splicing: The *Tetrahymena* L-16ScaI ribozyme reveals a new role for the G★U pair in self-splicing. *Biochemistry* **46,** 4861–4875.

Lakowicz, J. R. (2006). *Principles of Fluorescence Spectroscopy.* 3rd edn. Springer, New York.

LiCata, V. J., and Wowor, A. J. (2008). Applications of fluorescence anisotropy to the study of protein–DNA interactions. *Methods Cell Biol.* **84,** 243–262.

Rist, M. J., and Marino, J. P. (2002). Fluorescent nucleotide base analoges as probes of nucleic acid structure, dynamics and interactions. *Curr. Org. Chem.* **6,** 775–793.

Sandin, P., Wilhelmsson, L. M., Lincoln, P., Powers, V. E. C., Brown, T., and Albinsson, B. (2005). Fluorescent properties of DNA base analogue tC upon incorporation into DNA — negligible influence of neighbouring bases on fluorescence quantum yield. *Nucleic Acids Res.* **33,** 5019–5025.

Sandin, P., Lincoln, P., Brown, T., and Wilhelmsson, L. M. (2007). Synthesis and oligo-nucleotide incorporation of fluorescent cytosine analogue tC: A promising nucleic acid probe. *Nat. Protoc.* **2,** 615–623.

Sandin, P., Borjesson, K., Li, H., Martensson, J., Brown, T., Wilhelmsson, L. M., and Albinsson, B. (2008). Characterization and use of an unprecedently bright and structurally non–perturbing fluorescent DNA base analog. *Nucleic Acids Res.* **36,** 157–167.

Shi, X., Mollova, E. T., Pljevaljcic, G., Millar, D. P., and Herschlag, D. (2009). Probing the dynamics of the P1 helix within the *Tetrahymena* group I intron. *J. Am. Chem. Soc.* **131,** 9571–9578.

Thomas, J. C., Allison, S. A., Appellof, C. J., and Schurr, J. M. (1980). Torsion dynamics and depolarization of fluorescence of linear macromolecules. II. Fluorescence polarization anisotropy measurements of a clean viral phi 29 DNA. *Biophys. Chem.* **12,** 177–188.

Wilhelmsson, L. M., Holmen, A., Lincoln, P., Nielson, P. E., and Norden, B. (2001). A highly fluorescent DNA base analog that forms Watson-Crick base pairs with guanine. *J. Am. Chem. Soc.* **123,** 2434–2435.

Wilhelmsson, L. M., Sandin, P., Holmen, A., Albinsson, B., Lincoln, P., Norden, B., and Phys, J. (2003). Photophysical characterization of fluorescent DNA base analog, tC. *J. Phys. Chem. B* **107,** 9094–9101.

Wilson, J. N., and Kool, E. T. (2006). Fluorescent DNA base replacements: reporters and sensors for biological systems. *Org. Biomol. Chem.* **4,** 4265–4274.

Zhang, Q., Sun, X. Y., Watt, E. D., and Al-Hashimi, H. M. (2006). Resolving the motional modes that code for RNA adaptation. *Science* **311,** 653–656.

Zhang, Q., Stelzer, A. C., Fisher, C. K., and Al-Hashimi, H. M. (2007). Visualizing spatially correlated dynamics that directs RNA conformational transitions. *Nature* **450,** 1263–1267.